



OPEN Impact of seaweeds on tensile, thermal and viscoelasticity behavior of polybutylene adipate terephthalate-based composites

Muhamad Haikal Hamdan¹, Siti Noorbaini Sarmin¹, Zoheb Karim², Mohammad Jawaid²✉, Ahmad Safwan Ismail^{3,4} & Nurjannah Salim⁵

In the current study, a composite was produced using *Kappaphycus alvarezii* (*K. Alvarezii*) as filler with poly(butylene adipate-co-terephthalate) (PBAT). The varying concentrations of *K. Alvarezii* (10 wt%, 20 wt%, 30 wt%, and 40wt%) were used to determine their impact on the mechanical, thermal, morphological, and viscoelastic properties of the produced composites. Addition of *K. Alvarezii* particles to PBAT resulted in an improvement in the tensile modulus and decrease in the damping factor (Tan delta). An observed inverse correlation between the storage and loss modulus was analyzed. The thermogravimetric investigation demonstrated the degradation temperature of composites falls within the range of temperatures exhibited by their pristine components, i.e., *K. Alvarezii* and PBAT. As the amount of *K. Alvarezii* particles increased, improved melting (T_m) was observed. Indeed, *K. Alvarezii* serve as a filler to produce polymer composites which are environmentally friendly and possess enhanced capabilities. These biobased composites could be used in eco-friendly food packaging, pharmaceutical appliances, and several new green chemical applications.

Keywords *Kappaphycus alvarezii*, Poly(butylene adipate-co-terephthalate), Biopolymer, Tensile properties, Thermal properties

Poly(butylene adipate-co-terephthalate) (PBAT) have been successfully developed and brought to market by BASF and Eastman Chemical¹. These co-polyesters, known as Ecoflex and Easter-bio^{1,2}, are mainly derived from 1,4-butanediol, adipic acid, and terephthalic acid. They offer a customizable balance between biodegradability and desirable physical properties. Additionally, PBAT exhibits greater flexibility and better elongation at break compared to several other biodegradable polyesters, such as polylactic acid (PLA)³. One of the primary constraints hindering the broader adoption of PBAT in industrial and medical applications is its inadequate thermal and mechanical durability, which restricts its use in various fields. However, the limitations can be addressed by improving the thermal and/or mechanical qualities using filling techniques⁴. Furthermore, it was also discussed in the literature that PBAT could also be used as matrix for the fabrication of composites. In this context, SnO₂ nanoparticles used as reinforcement agent with PBAT for the fabrication of composites with improved antibacterial properties⁵. Some other active compounds used with PBAT composites are ZnO⁶, gallic acid⁷, SiC/g-C₃N₄ hybrid⁸, SiO₂⁹, carbon nanoparticles¹⁰, C₃N₄/TiO₂ hybrids¹¹, Fe₃O₄¹², and TiO₂¹³.

Research has also shown that incorporating nano-sized fillers into polymers can potentially provide them with multiple functional features, such as improved magnetic, catalytic, optical, electrical, thermal, and mechanical characteristics compared to traditional formulations of the same material². According to Xie et al.¹⁴ when compared to pure PBAT, the composites have shown a greater degree of mass loss, reduced thermal stability, higher melting point, lower crystallinity during deterioration, increased modulus and flexural strength, and a considerable rise in heat deflection temperature after blending with reed filler. In another

¹Department of Wood Technology, Faculty of Applied Science, Universiti Teknologi MARA, 26400 Jengka, Pahang, Malaysia. ²Department of Chemical and Petroleum Engineering, College of Engineering, United Arab Emirates University (UAEU), Al Ain, UAE. ³Chemical Engineering Programme, Faculty of Engineering, Universiti Malaysia Sabah, Jalan UMS, 88400, Kota Kinabalu, Sabah, Malaysia. ⁴Faculty of Industrial Sciences and Technology, Universiti Malaysia Pahang, Lebuhraya Tun Razak, Gambang, 26300 Kuantan, Pahang, Malaysia. ⁵Department of Bio-Composite Laboratory, Institute of Tropical Forestry and Forest Products, University Putra Malaysia, 43400 UPM Serdang, Selangor, Malaysia. ✉email: jawaid@uaeu.ac.ae

study by Techawinyutham et al.¹⁵, the mechanical properties, thermal stability, and natural dark colouring of the bio-composite can be enhanced using mangosteen peel and durian peel as bio pigments and natural reinforcement materials in biopolymer PBAT matrix. These materials are suitable for use in environmentally friendly alimentary packaging and pharmaceutical zipper bagging. Furthermore, Kong et al.¹⁶ have discovered the tensile characteristics of the PBAT composite films. The composite films achieved their highest values when containing 7 wt% of cellulose nanofibril (CNFs), exhibiting a tensile strength of 6.2 MPa and an elastic modulus of 263 MPa. The values exhibited 59% and 180% augmentation, respectively, in comparison to the composition without NFC. Nevertheless, the characteristics of polymers, including thermal, electrical, and barrier properties, can also be influenced by the specific type of filler used.

Despite the abundance of research articles exploring the incorporation of algae into polymer matrices, there is a lack of research specifically focused on PBAT reinforced *Kappaphycus alvarezii* bio-fillers. *K. Alvarezii* is the most extensively cultivated seaweed because of its status as a critical source of carrageenan, which is extensively used in the food industry¹⁷. The utilisation of *K. Alvarezii* biomass has been utilised in the fabrication of biofilms¹⁸, as well as in the advancement of biofuels and nanomaterials¹⁹, specifically for the food packaging sector²⁰.

Thus, in this study, raw seaweed i.e., *K. Alvarezii*. *K. Alvarezii* is tested as a filler for the fabrication of PBAT based composite, in depth, to test our hypothesis regarding the impact of *K. Alvarezii* on final properties of produced composite, various percentages of *K. Alvarezii* (10 to 40%) was used for the production of PBAT based composites and the impact of this biofiller was tested for mechanical and viscoelastic behaviours of produced composites. This study utilised *K. Alvarezii*, a cost-effective and eco-friendly carbohydrate source, as a filler for PBAT. The thermal and viscoelastic characteristics of the developed composites were analysed using the thermogravimetric (TGA), differential scanning calorimeter (DSC), and dynamic mechanical analyser (DMA). The properties investigated included storage modulus (E'), loss modulus (E''), Tan delta ($\tan \delta$) and glass transition temperature (T_g). Furthermore, the composites' surface microstructures and tensile strength properties were analysed. The composite developed through this research will provide a novel approach for the creation of completely eco-friendly materials.

Experimental work

Preparation of raw materials

The PBAT (EcoFlex® F Blend C1200) used in this study was obtained from BASF Industry Co., Ltd., situated in Ludwigshafen, Germany. The melt flow index (MFR) ranged from 2.7 to 4.9 g/10 min under a temperature of 190 °C and a weight of 2.16 kg. The material had a density realm of 1.25 to 1.27 g/cm³, with a melting temperature falling within the range of 110 to 120 °C.

The seaweed, *K. Alvarezii*, was provided by Green Leaf Synergy Sdn. Bhd. which was in Tawau, Sabah, Malaysia. The seaweed was rinsed with distilled water and then dried in an oven at a temperature of 80 °C for a duration of 24 h. The dried seaweed was crushed into a fine powder, sieved using a vibrating sieve shaker, and then stored in zip-lock containers. The dried seaweed has an average particle size ranging from 100 to 150 micron and its moisture content varies between 3 to 5%. No further chemical purification was performed after getting the power of seaweed.

Fabrication of composites

The PBAT/seaweed mixtures were produced by initially preparing a master batch of pure PBAT in a Rheomixer, which was operated at a temperature of 110 °C and a speed of 60 rpm. The master batch was mixed with different ratios of seaweed: 0wt% (PBAT), 10wt% (SW10), 20wt% (SW20), 30wt% (SW30), and 40wt% (SW40). The PBAT/seaweed blend was subsequently crushed into pellets approximately 1–3 cm in length. 300 × 300 × 3 mm size sample was prepared by compression molding using a laboratory press at a temperature of 100 °C for 180 s, under the pressure of 100 bar.

Characterization

Tensile strength test

The tensile strength of the samples (Fig. 1) was evaluated using the Blue Hill Instron Universal Testing Machine (UTM) in accordance with the ASTM D638 Type IV standard. The samples were dumbbell-shaped (dogbone) in shape, measuring 115 mm (L) × 19 mm (W) × 3 mm (T), and five replicates were tested. Initially, the samples were securely fastened to the pneumatic jaw of the Universal Testing Machine (UTM) at a precise spacing of 30 mm. A load cell with a capacity of 5 kN was mounted on the testing equipment. Testing was conducted with a crosshead speed of 1 mm/min for 1 min, then raised to 100 mm/min automatically until the sample fractured, considering the significant elongation of the samples being tested.

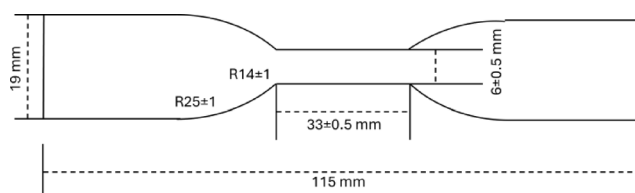


Fig. 1. The dimensions of sample taken for mechanical testing.

Dynamic mechanical analysis (DMA)

The viscoelastic properties of the samples were determined using the Dynamic Mechanical Analysis instrument, namely the TA Q-800. The samples were assessed according to ASTM D4065²¹ and they were rectangular in shape with dimensions of 60 mm in length, 12.5 mm in width, and 3 mm in thickness. The experiment was conducted under a nitrogen atmosphere using the three-point bending mode. The temperature scan ranged from 30 to 150 °C, with a frequency of 1 Hz. The heating rate was set at 10 °C/min till reaching 150 °C. The storage modulus (E) and mechanical loss factor ($\tan \delta$) were determined as a function of temperature during the test.

Thermogravimetric analysis (TGA)

The composite's thermal establishment was examined adopting thermogravimetric analysis (TGA) following the guidelines of ASTM E1131-03²¹. The TGA analysis of all materials was conducted using the Mettler TGA Q 500 TA instrument, with scanning performed under a nitrogen environment at a flow rate of 50 ml/min. The samples, which weighed between 40 and 45 mg, were fixed in an alumina container and heated to various temperatures ranging from 30 to 800 °C at a rate of 10 °C per minute.

Differential scanning calorimeter (DSC)

The differential scanning calorimetry was conducted using a Mettler Toledo DSC 822e instrument, alongside a flow rate of 50 mL/min and a heating rate of 10 °C/min, in a nitrogen atmosphere. The samples were accommodated in an alumina crucible and subjected to scanning between 50 and 300 °C, with an approximate sample weight of 30 to 40 mg.

Scanning electron microscopy (SEM)

The composite samples were coated with gold adopting an electro deposition process to help them conduct electricity. The morphology of the materials was analysed using an EM-30AX scanning electron microscope (COXEM, Daejeon, Korea) with an operating voltage of 2 kV.

Sample partition and moisture analysis

Previously dried seaweed sample were grounded with a food-grade miller to decrease the particle size. The ground samples were sieved on a Sieve shaker (Retsch As 200, UAE) to separate the samples into size in between 100 and 150 μm . The dried samples with this particle size were used for the fabrication of composites.

Furthermore, the moisture content in the seaweed particles was measured using conventional methods, the weight of seaweed was measured and then dried at 95 °C for 24 h and then the percentage weight loss after drying was measured. The percentage moisture of samples was calculated as given below (Eq. 1).

$$\% \text{ moisture content} = \frac{\text{weight before dry} - \text{weight after dry}}{\text{weight before dry}} \times 100 \quad (1)$$

Results and discussion

Tensile properties

Figure 2 portrays the histogram representing all tensile properties of PBAT/seaweed specimens. All in the composite materials exhibit a linear decrease in the tensile strength (Fig. 2a) and increase tensile modulus (Fig. 2b) with the increased content of the seaweed filler concentration. Conversely, the presence of *K. Alvarezii* causes a reduction in the tensile strength (Fig. 2a) of all the specimens. SW40 exhibits a decrement in tensile strength of approximately 50% when compared to pure PBAT. The reduction in the tensile strength of the composite is perhaps attributed to the early failure of the specimens, which is anticipated when inflexible

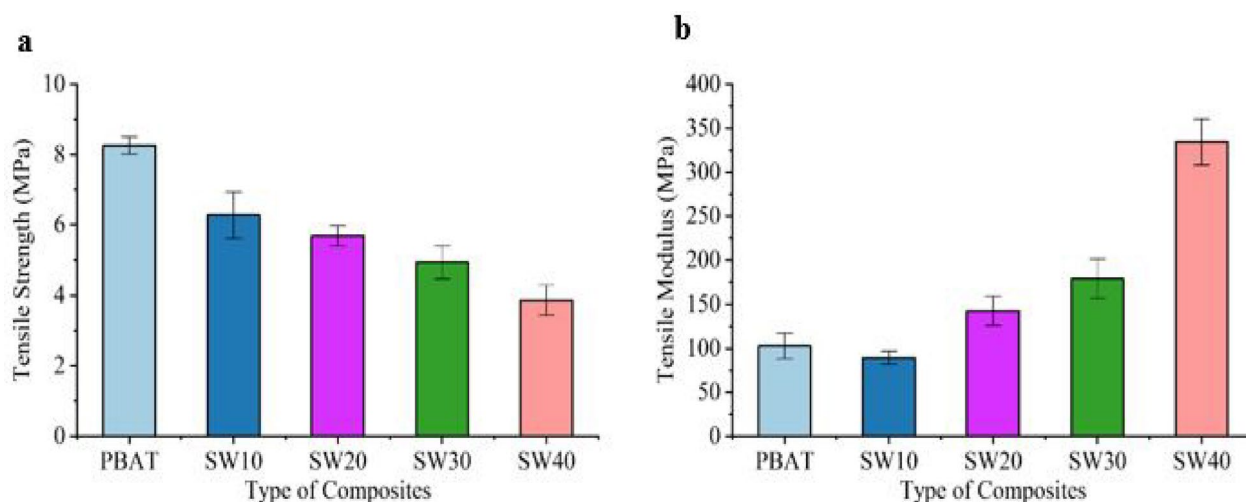


Fig. 2. (a) tensile strength and (b) tensile modulus of PBAT/seaweed composite.

particles are added to the polymer matrix. This is because the interface between the filler and matrix, inclusive of the presence of voids, can serve as defects in the composites. Furthermore, the inclusion of *K. Alvarezii* particles may have modified the arrangement of PBAT polymer chains inside the crystal lattice, leading to a decrease in the crystallinity of the mix thus causing a decline in tensile strength. Comparable outcomes have been observed for PBAT composites reinforced with organic synthetic, and lignocellulosic particle, where significant decrease in the tensile strength was calculated after increase concentration of filler and high modulus was determined of composite having high percentage of filler^{22–24}.

Furthermore, in the literature, the *K. Alvarezii* has 12.69 ± 0.6 to 23.61 ± 0.02 g/100 g DW of protein fraction and between 9.68 ± 0.08 and 18.57 ± 0.15 g/100 g DW of fiber. The lipid content was the lowest among the constituents investigated (0.39 ± 0.04 to 0.91 ± 0.51 g/100 g DW). Total mineral content ($29,939.61 \pm 9340.38$ mg/100 g DW). The Na/K ratio during the study ranged from 0.34 to 0.87²⁵. It is further mentioned in the literature²⁶ that the impact of proteins and fibers is the highest during composite production, and these two constituents have direct impact on the final properties of formed composite. The decrease in the tensile strength after increasing the concentration of *K. Alvarezii* is understood. As mentioned in the literature, at low loading of blue algae, the relevant low shear stress indicated by low viscosity, might not be able to sufficient deform the algae phase, thus, algae displayed less stretching and reduction in size. At higher content, the fractured surface was composed of relatively smaller elliptical granules of algae, which was presented as islands in the sea of continuous PBSA phase. The interstices between PBSA matrix and the blue algae granules were apparently observed, indicating the interfacial adhesion was weak²⁷.

Specifically, the tensile modulus of PBAT significantly increases from 98 up to 147 MPa, 172 MPa, and 381 MPa for SW20, SW30 and SW40 respectively. To elaborate further, the tensile modulus demonstrates a notably elevated value when 40wt% (SW40) of *K. Alvarezii* is employed as reinforcement. The increment of tensile moduli observed for the samples may be due to the transfer of part of stresses to the disperse phase. Furthermore, the stress concentration zones around *K. Alvarezii* particles intensify as their proximity increases at elevated concentrations. The acquired results might be viewed as further confirmation of the positive interaction between the phases present in the composite. The initial decline observed in SW10 may be attributed to an insufficient quantity of *K. Alvarezii*, which only disrupts the PBAT structure without being able to accumulate stresses.

Dynamic mechanical analysis (DMA)

Figure 3 illustrates the relationship between the storage modulus E' and temperature for both neat PBAT and PBAT/seaweed composites, measured at a frequency of 1 Hz. The initial temperature range observed is between -40 to -30 °C, which indicates the stiffness of the matrix at low temperature (glassy state). The sample containing 20wt% *K. Alvarezii* exhibits a greater value of E' (1937 MPa) compared to the samples with 40wt% (1791 MPa), 10wt% (1690 MPa), and 30wt% (1156 MPa) in the early state. It is frequently noticed that many polymers have a clearly defined plateau below the glass transition temperature (T_g)²⁸. The presence of *K. Alvarezii* on this plateau tends to partially obscure or conceal the reinforcing effect. The presence of filler effect is consistently seen in PBAT matrix, regardless of the type of filler or processing approached used^{29,30}.

At elevated temperatures, both PBAT and seaweed experience a reduction in stiffness, leading to a fall in the storage modulus. It is noteworthy that composites reinforced with 10wt%, 20wt%, 40wt%, and pure PBAT have a more significant reduction in the value of E' as the temperature rises, in contrast to composites containing 30wt% *K. Alvarezii*. The second and third segments of the curves, which occur at temperatures ranging from -20 to 10 °C, are linked to polymer relaxation. This precedence to a substantial decline in the material's storage

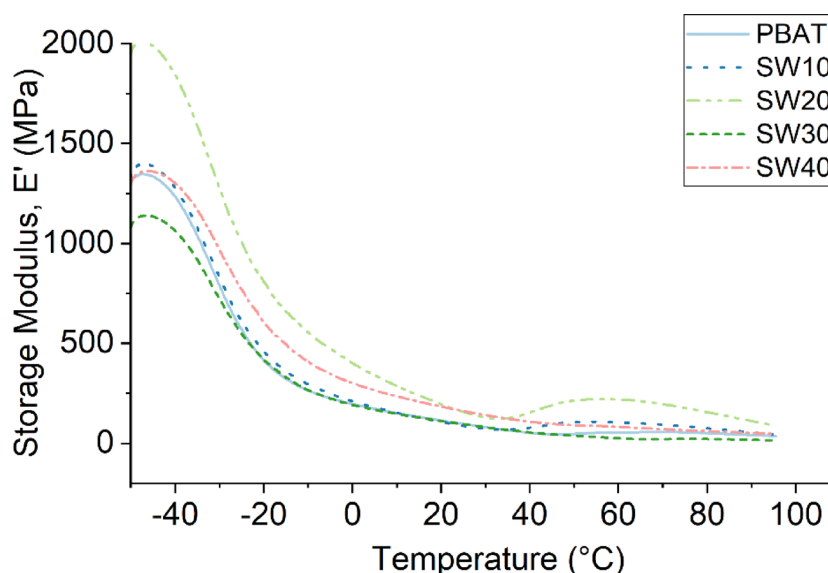


Fig. 3. Storage modulus results of PBAT/seaweed. The observed trends are statically significant.

modules. The weakening of the polymeric matrix in both regions resulted in a more pronounced reinforcing effect of the *K. Alvarezii*. The storage modulus of composites containing 20% by weight is determined to be around 28.7 MPa at a temperature of roughly 100 °C. The figure is markedly greater than the storage moduli of the other composites (10% weight: 24.4 MPa, 40% weight: 24.4 MPa) and pure PBAT (19.2 MPa). Aftereffect, the inclusion of *K. Alvarezii* has a negligible outcome on the E' value of the composites in the plastic region. This trend validates that a concentration of 20wt% improves the compatibility between the PBAT polymer, which is used as the matrix. It is further noted that greater reduction of storage module of 30wt% composite might be due to the insufficient interfacial addition of filler with PBAT, the trend is very close to the pristine-PBAT (0 to 50 °C). Furthermore, the SEM images shown in Fig. 8d, supported this explanation, the greater defects can be seen in the image compared to other produced composites.

The loss modulus E'' corresponds to the material's viscous behaviour²⁹. The symbol E'' represents the viscous response of the substance. Figure 4 illustrates the variations in E'' in PBAT and PBAT/seaweed composites with respect to temperature. The data clearly indicates that the loss modulus of all materials demonstrates an escalation in the plastic zone (−40 to −30 °C) followed by a decline in the elastic region (−20 to 10 °C) as the temperature increases. Observations have shown that the presence of *K. Alvarezii* affects the value of E'' , both below and raised the glass transition temperatures (the temperatures at which E'' achieves its highest values). The loss modulus of PBAT is found to be lower than that of the reinforced composites in both the plastic and rubbery area. More precisely, the addition of *K. Alvarezii* increases the loss modulus of composites at high temperatures.

The study also examines the relaxation of the polymer and the influence of *K. Alvarezii* by analyzing the peak in the mechanical loss factor (Tan delta, Fig. 5). The damping curves of the samples are similar, suggesting that there is a limited interaction between *K. Alvarezii* and PBAT. The presence of *K. Alvarezii* particles causes a decrease in the height of the tan delta peak. The absence of any constraints on the chain movement in the pure PBAT matrix is the reason for this phenomenon. However, the inclusion of *K. Alvarezii* particles restricts the mobility of the chains, ensuing in a decrement in the sharpness and height of the tan delta peak. The Tg values obtained from the tan delta peak for a variety of samples are also depicted in Fig. 5. The values obtained agree with those reported in the literature^{27–29} and demonstrate a correlation with the *K. Alvarezii* content. The occurrence of two thermal transitions (Tg) can be attributed to the aliphatic and aromatic components of PBAT, respectively. Furthermore, in literature, brown seaweed *Sargassum spp*, was used as filler to produce composites. The DMA studies performed and the comparative study was evaluated in the article³¹. The same pattern of Tan delta was evaluated as mentioned in the current study. Furthermore, our findings are also supported by the other published articles, where decrease in tan delta was observed after increase in the filler content^{32,33}. Furthermore, in an article, four composites were produced using PBAT and their tan delta curve was analyzed, a shift in peaks after addition of filler was seen in each composites, furthermore, stipulates the glass transition temperature of −20 °C for neat PBAT, and the incorporation of filler particles causes the curve of each composite to shift to the right, indicating a higher glass transition temperature compared to neat PBAT³⁴ but in the current study, no such transition was recorded with increasing percentage of filler addition, thus, no impact on shift in glass temperature was recorded in current study.

Thermogravimetric analysis (TGA)

Table 1 and Fig. 5 report the thermal stability impact of *K. Alvarezii* filled in PBAT. In this study, we present the derivative of the TGA curves and the accompanying inset. Table 1 provides the temperature at which deterioration

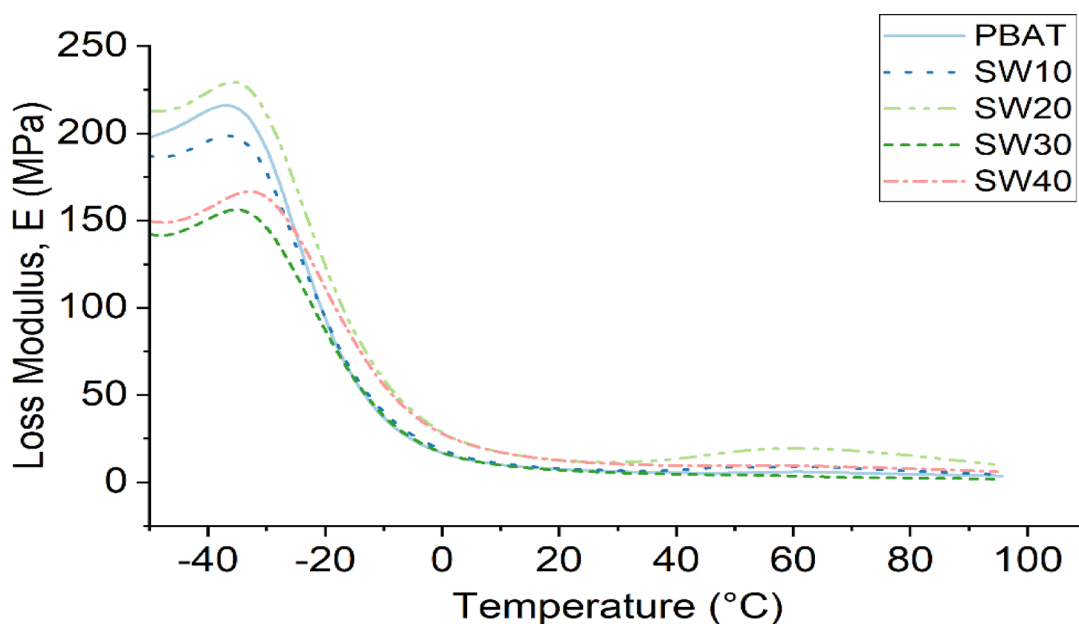


Fig. 4. Loss modulus results of PBAT/seaweed. The observed trends are statically significant.

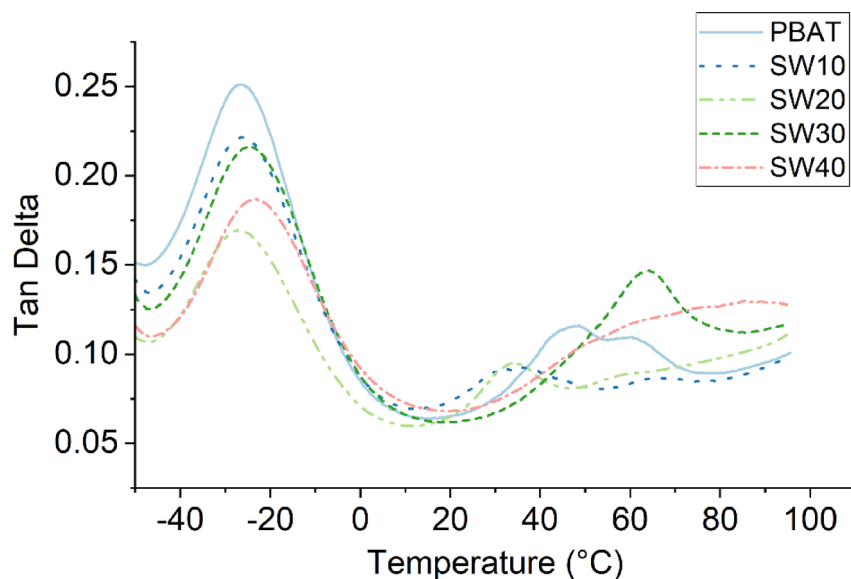


Fig. 5. Tan delta results of PBAT/seaweed. The observed trends are statically significant.

Type of Composites	T at 5%	T at 25%	T at 50%	T at 75%	Residue at 600 °C (%)
PBAT	360.43	392.61	405.67	417.16	3.46
SW 10	182.38	376.78	404.30	463.05	19.91
SW 20	180.77	374.54	403.72	434.12	19.99
SW 30	186.96	378.54	403.90	430.97	16.91
SW40	189.63	381.23	409.85	433.62	20.56

Table 1. Thermal characteristics of PBAT/seaweed from TGA thermogram. *Temperatures are given based on total weight lost at 5%,25%,50% and 75%

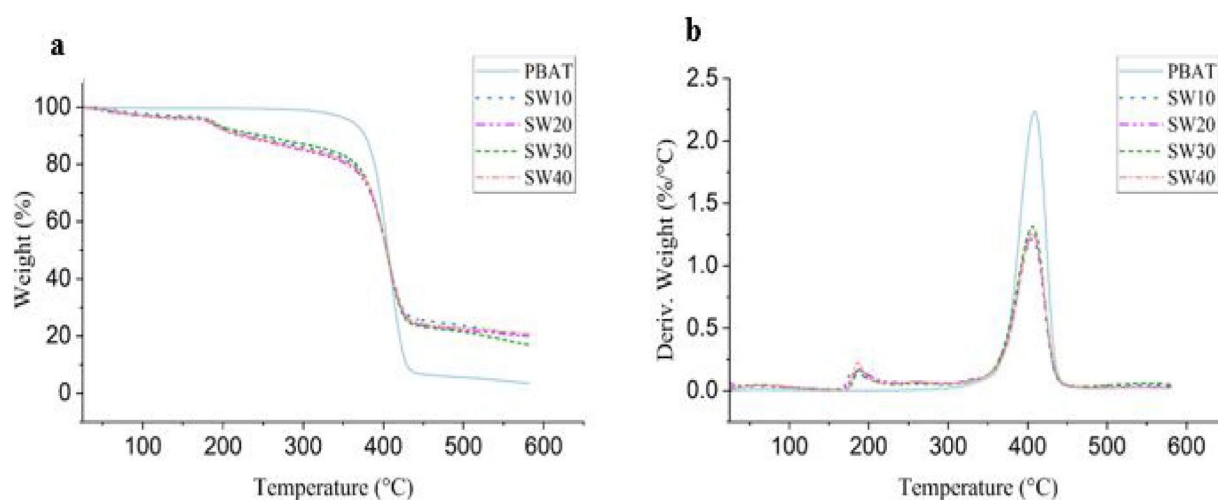


Fig. 6. (a) TGA and (b) DTG curves of PBAT/seaweed. The observed trends are statically significant.

takes place and leads to weight loss of 5%, 25%, 50%, and 75%. The TGA curves of pure PBAT, as depicted in Fig. 6a, demonstrate a single-stage primary weight loss of the PBAT matrix at a temperature of 383 °C. The PBAT/seaweed composites exhibit two distinct degradation phases due to the destruction of *K. Alvarezii* particles. As the *K. Alvarezii* concentration increases, the decomposition temperature of the composites oscillates towards the decomposition temperature of *K. Alvarezii*. To facilitate accurate observation, several temperature ranges of deterioration are identified in the DTG plot, as shown in Fig. 6b. The initial stages of weight reduction occurred

within the temperature range of 100 to 380 °C and are primarily attributed to the presence of *K. Alvarezii*, likely associated with the breakdown of galactose units. Subsequently, the sample exhibits a gradual decrease in weight, which has been ascribed to the additional fragmentation of the composition products from the second phase. The ash concentration of the residual material at a temperature of 600 °C is approximately 19% by weight. The last weight loss seen between 350 and 450 °C corresponds directly to the thermal degradation of PBAT.

The degradation temperature (peak values) of the specimens at weight loss of 5% ($T_{5\%}$), 25% ($T_{25\%}$), 50% ($T_{50\%}$), and 75% (T_{max}), as well as the residual weight loss at 600 °C, are shown in Table 1. The intermediate degradation temperature readings indicate a recurring synergy amid the *K. Alvarezii* and PBAT matrix. PBAT exhibits the greatest thermal stability. The thermal stability of PBAT/seaweed composites decrease as the amount of *K. Alvarezii* increases, primarily because of the seaweed's low thermal degradation. The thermal stability of PBAT/seaweed composite follows a sequence: SW40 > SW30 > SW10 > SW20. The increase in *K. Alvarezii* concentration increases the residue char of the composites.

Differential scanning calorimeter (DSC)

The thermal characteristics of the polymer were examined by the analysis of the PBAT/seaweed composite using Differential Scanning Calorimetry (Fig. 7), to evaluate the influence of *K. Alvarezii* on these parameters. The DSC thermograms show a melting endotherm, indicating the fusion of the PBAT matrix. This peak has a lower elevation and is slightly broader in comparison to the other thermograms. The melting temperature exhibits a small increase as the *K. Alvarezii* concentration increases. This phenomenon may arise from intermolecular interactions occurring between the *K. Alvarezii* particles and PBAT chains, resulting in the formation of thinner lamellar crystals. The hydrogen bond alliance amid the carbonyl units of PBAT and the hydroxyl, sulphate, and glycosidic groups of *K. Alvarezii* is anticipated. These interactions take place in the amorphous state, where they have a reduced impact on the degree of crystallisation compared to PBAT domains. Figure 7 demonstrates that the inclusion of *K. Alvarezii* act as a nucleating agent, increasing the crystallization temperature (T_c) of the composites. This behavior indicates that *K. Alvarezii* functions as a nucleation agent and causes PBAT crystallization. The nucleation outcome is further evident with increasing amounts of *K. Alvarezii*, as a higher quantity of *K. Alvarezii* resulted in a greater number of heterogeneous nuclei for crystallization.

Scanning electron microscopy (SEM)

Figure 8 showcases selected photos illustrating the geometric nature of the composites' surfaces. The photos depict the samples of (a) PBAT, (b) SW10, (c) SW20, (d) SW30, and (e) SW40, respectively. Figure 8a illustrates that the surface of the neat PBAT is significantly smoother compared to the other samples. The photos demonstrate that the visible amount of *K. Alvarezii* rises proportionally with the increase in filler volume fraction. In addition, the seaweed particles are evidently evenly distributed throughout the PBAT matrix, furthermore, the clear gaps/defects can be easily seen after increase in the filler content. The increase in the defect with increase in the filler content could be due to the inhomogeneous distribution of filler during the composite production. The images are also in the support of obtained tensile strength (Fig. 2a), which indicate the decrease in nature after increase the filler content. The significant decrease in the tensile strength could be due to the increase in defects after addition of filler. The same finding was also reported in recent published article where brown algae was used as filler for the production of composites. Adding 6 wt.% brown algae filler in the jute fiber composite enhanced the tensile strength by 34.39 MPa and improved the impact strength to 101.24 J/m². There is a 73.16 MPa increase in flexural strength and 47.45 MPa shear strength in the brown algae-filled jute fiber polymer composites. When

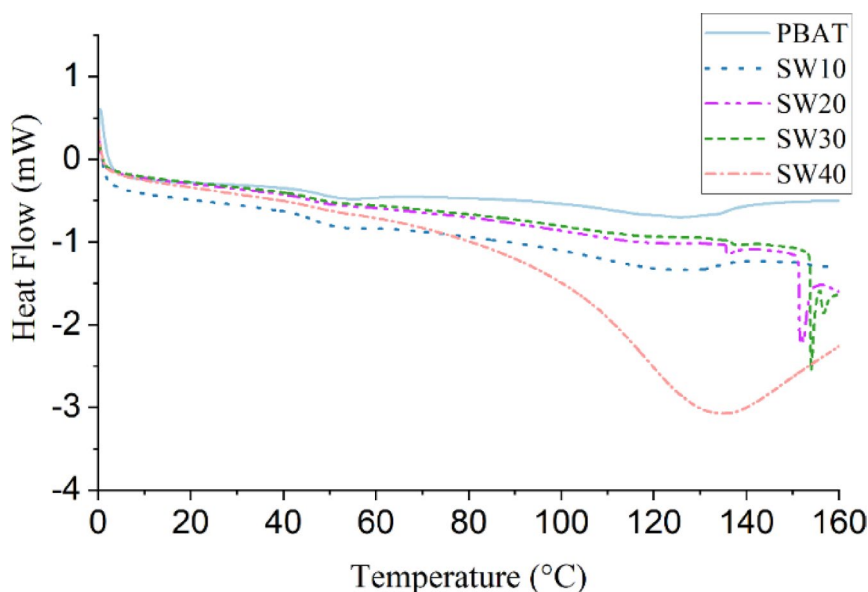


Fig. 7. DSC thermograms of PBAT/seaweed. The observed trends are statically significant.

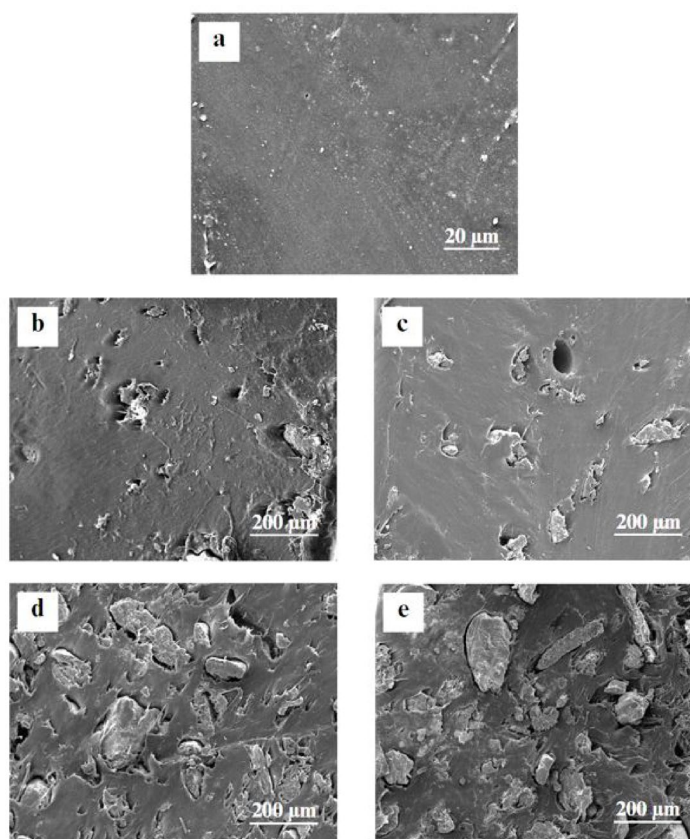


Fig. 8. SEM micrograph with magnification of 100× of PBAT/seaweed. The images are named as (a) PBAT, (b) SW10, (c) SW20, (d) SW30, and (e) SW40.

Filler type	Matrix	Tensile strength (MPa)	Tensile Modulus (MPa)	TGA analysis		Ref
				Weight loss at 50 °C	Total remaing residues at 600 °C	
Seaweed	10%	7.1	100	404.30	19.91	Current study
	40%	4.2	350	409.85	20.56	
TiO ₂	PBAT	3.6	369	308.78	NA	³⁹
Corn based bioparticles		NA	NA	234.57	6.67	⁴⁰
Wine waste bioparticle		NA	NA	245.67	3.45	
Lignin nanoparticles		13	200	456.67	NA	³⁷
PLA		14	300	236.45	2.35	³⁸

Table 2. A state of the art of produced PBAT based composites and their comparative study.

the brown algae filler content in the jute fiber is above 6 wt.%, the mechanical properties of the jute polymer epoxy composite are reduced³⁵. Indeed, the same results are also reported in another publications³⁶.

State of the art

Furthermore, the results obtained in the current study are compared with the literature. As shown in Table 2, various PBAT based composites reported in the literature are reported in Table 2 and the two main properties reported using mechanical and viscoelastic are compared. The minimum and maximum percentage of seaweed i.e. 10% and 40% base composite were tested, and the tensile strength and modulus were 7.1 and 100 MPa, respectively. The TiO₂ composite with PBAT was fabricated by Sciancalepore et al.³⁹ and lower tensile strength but higher module i.e., 3.6 MPa and 308.78 MPa was reported. Furthermore, the weight loss at 50 °C was lower compared to composite present in current study (Table 2). In another study, biobased composite was prepared and weight loss was detected using TGA, indeed, low weight loss at 50 °C (234.57 and 245.67) was recorded compared to current study. Lignin nanoparticles were used as filler for the fabrication of composite, very high

tensile strength and modulus compared to current study were recorded. Furthermore, higher weight loss was also recorded³⁷. In another study, polylactic acid (PLA) based composite was prepared and the mechanical property was measured, High tensile strength (14 MPa) and moderate modulus (300 MPa) were recorded using tensile tester, in addition less weight loss was calculated using TGA³⁸.

Conclusions

The study shows that incorporating *K. Alvarezii* particles into PBAT led to an increase in tensile modulus. The DMA tests disclosed that the addition of *K. Alvarezii* resulted in an augmentation of the storage modulus, indicating an enhancement in rigidity. However, the T_g computed adopting the loss modulus peak of DMA spectra revealed a minor variation. This phenomenon could be ascribed to the limited maneuverability of polymer chains in proximity. The TGA outcome demonstrated that the thermal stability of PBAT/seaweed composites was moderate in comparison to their separate constituents. The inclusion of *K. Alvarezii* particles in the composites led to a reduction in the degree of crystallinity and an elevation in both melting temperature (T_m) and crystallization temperature (T_c), as indicated in the DSC tests. The rheological properties of PBAT/seaweed composites suggested that the *K. Alvarezii* particles exhibited movement within the polymeric matrix under specific velocity conditions. The scanning electron microscope (SEM) analysis showed that the *K. Alvarezii* particles were well-dispersed and interacted effectively with the matrix, as evidenced by their behaviour under dynamic conditions. Cryogenically fractured surfaces displayed a smooth form, with *K. Alvarezii* particles encapsulated within the PBAT matrix. The potential cause can be ascribed to the extent of adhesiveness between *K. Alvarezii* and PBAT. Furthermore, the obtained properties were further compared with the available literature when various fillers were used for the fabrication of composite with PBAT. Indeed, some properties of the current composite are better, and some are not.

Data availability

Data can be obtained on request from Corresponding author (M. Jawaid).

Received: 16 December 2025; Accepted: 30 January 2026

Published online: 09 February 2026

References

- Ratshoshi, B. K., Farzad, S. & Görgens, J. F. A techno-economic study of Polybutylene adipate terephthalate (PBAT) production from molasses in an integrated sugarcane biorefinery. *Food Bioprod. Process.* **145**, 11–20 (2024).
- Pandey, K., Antil, R., Saha, S., Jacob, J. & Balavairavan, B. Poly(lactic acid)/thermoplastic polyurethane/wood flour composites: Evaluation of morphology, thermal, mechanical and biodegradation properties. *Mater. Res. Express* **6**, 125306 (2019).
- Ma, J. et al. Degradation characteristics of polybutylene adipate terephthalic acid (PBAT) and its effect on soil physicochemical properties: A comparative study with several polyethylene (PE) mulch films. *J. Hazard. Mater.* **456**, 131661 (2023).
- Dmitruk, A., Ludwiczak, J., Skwarski, M., Makula, P. & Kaczyński, P. Influence of PBS, PBAT and TPS content on tensile and processing properties of PLA-based polymeric blends at different temperatures. *J. Mater. Sci.* **58**, 1991–2004 (2023).
- Venkatesan, R. & Rajeswari, N. Poly(butylene adipate-co-terephthalate) bionanocomposites: Effect of SnO₂ NPs on mechanical, thermal, morphological, and antimicrobial activity. *Adv. Composit. Hybrid Mater.* **1**, 731–740 (2018).
- Venkatesan, R. & Rajeswari, N. ZnO/PBAT nanocomposite films: Investigation on the mechanical and biological activity for food packaging. *Polym. Adv. Technol.* **28**, 20–27 (2017).
- Hou, T. et al. Enhancing cherry tomato packaging: Evaluation of physicochemical, mechanical, and antibacterial properties in tannic acid and gallic acid crosslinked cellulose/chitosan blend films. *Int. J. Biol. Macromol.* **285**, 138276 (2025).
- Venkatesan, R. et al. Development of PBAT films reinforced with SiC/g-C₃N₄ nanohybrids for enhanced biocompatibility and antibacterial performance. *Scientif. Rep.* **16**, 2326 (2025).
- Venkatesan, R. & Rajeswari, N. Preparation, mechanical and antimicrobial properties of SiO₂/ Poly(butylene adipate-co-terephthalate) films for active food packaging. *SILICON* **11**, 2233–2239 (2016).
- Venkatesan, R. et al. Biodegradable composites from poly(butylene adipate-co-terephthalate) with carbon nanoparticles: Preparation, characterization and performances. *Environ. Res.* **235**, 116634 (2023).
- Venkatesan, R. et al. Poly(butylene adipate-co-terephthalate) packaging films with g-C₃N₄/TiO₂ hybrids: Enhancing shelf life of fresh-cut apples. *J. Environ. Chem. Eng.* **13**, 119194 (2025).
- Venkatesan, R., Kamaraj, E., Mayakrishnan, V., Alrashed, M. M. & Kim, S. C. Advanced PBAT/Fe₃O₄ nanocomposite films for extending the shelf life of cherry tomatoes. *Food Chem.* **496**, 146837 (2025).
- Venkatesan, R., Dhilipkumar, T., Kiruthika, A., Ali, N. & Kim, S. C. Green composites for sustainable food packaging: Exploring the influence of lignin-TiO₂ nanoparticles on poly(butylene adipate-co-terephthalate). *Int. J. Biol. Macromol.* **277**, 134511 (2024).
- Xie, L. et al. Effect of large sized reed fillers on properties and degradability of PBAT composites. *Polym. Compos.* **44**, 1752–1761 (2023).
- Techawinyutham, L., Techawinyutham, W., Rangappa, S. M. & Siengchin, S. Lignocellulose based biofiller reinforced biopolymer composites from fruit peel wastes as natural pigment. *Int. J. Biol. Macromol.* **257**, 128767 (2024).
- Kong, Y., Qian, S., Zhang, Z. & Tian, J. The impact of esterified nanofibrillated cellulose content on the properties of thermoplastic starch/PBAT biocomposite films through ball-milling. *Int. J. Biol. Macromol.* **253**, 127462 (2023).
- Rakhasiya, B. et al. Potential utility of industrially unwanted constituent under the framework of waste to wealth: Edible salt from commercial marine red seaweed *Kappaphycus alvarezii* (Doty) L.M. Liao. *Bioresour. Technol. Rep.* **23**, 101529 (2023).
- Nunes, A. et al. Uses and applications of the red seaweed *Kappaphycus alvarezii*: A systematic review. *J. Appl. Phycol.* **36**, 3409–3450 (2024).
- Rudke, A. R., Zanella, E., Stambuk, B. U., de Andrade, C. J. & Ferreira, S. R. S. Deconstruction of *Kappaphycus alvarezii* biomass by pressurized solvents to increase the carrageenan purity. *Food Hydrocoll.* **155**, 110204 (2024).
- Rajasekar, V., Karthickumar, P., Rose, A. H. R., Manimahalai, N. & Subhasri, D. Development and characterization of biodegradable film from marine red seaweed (*Kappaphycus alvarezii*). *Pigm. Resin Technol.* **52**, 478–489 (2023).
- Yoon Park, S. & Jong Choi, W. Review of material test standardization status for the material qualification of laminated thermosetting composite structures. *J. Reinf. Plast. Composit.* **40**, 235–258 (2021).
- Sheng, S. et al. Using sodium linoleate as a nucleating agent to improve the properties of PBAT/CaCO₃ composites. *J. Therm. Anal. Calorim.* **148**, 13859–13868 (2023).

23. Botta, L. et al. PBAT based composites reinforced with microcrystalline cellulose obtained from softwood almond shells. *Polymers* **13**, 2643 (2021).
24. Kargarzadeh, H., Galeski, A. & Pawlak, A. PBAT green composites: Effects of Kraft lignin particles on the morphological, thermal, crystalline, macro and micromechanical properties. *Polymer (Guildf)*. **203**, 122748 (2020).
25. Kumar, A., Hart, P. & Thakur, V. K. Seaweed based hydrogels: extraction, gelling characteristics, and applications in the agriculture sector. *ACS Sustain. Resour. Manag.* **1**, 1876–1905 (2024).
26. Beaumont, M. et al. Hydrogel-forming Algae Polysaccharides: from seaweed to biomedical applications. *Biomacromol* **22**, 1027–1052 (2021).
27. Lahaye, M. & Robic, A. Structure and functional properties of Ulvan, a polysaccharide from green Seaweeds. *Biomacromol* **8**, 1765–1774 (2007).
28. Ferreira, F. V., Lona, L. M. F., Pinheiro, I. F., de Souza, S. F. & Mei, L. H. I. Polymer composites reinforced with natural fibers and nanocellulose in the automotive industry: A short review. *J. Composit. Sci.* **3**, 51 (2019).
29. Olonisakin, K. et al. Fiber treatment impact on toughness and interfacial bonding in epoxidized soya bean oil compatibilized PLA/PBAT bamboo fiber composites. *Mater. Today Commun.* **38**, 107790 (2024).
30. da Costa, F. A. T., Parra, D. F., Cardoso, E. C. L. & Güven, O. PLA, PBAT, cellulose nanocrystals (CNCs), and their blends: Biodegradation, compatibilization, and nanoparticle interactions. *J. Polym. Environ.* **31**, 4662–4690 (2023).
31. Bauta, J. et al. Development of a binderless particleboard from Brown Seaweed *Sargassum* spp.. *Materials* **17**, 539 (2024).
32. Matusiak, J. et al. Textural and thermal properties of the novel fucoidan/nano-oxides hybrid materials with cosmetic, pharmaceutical and environmental potential. *Int. J. Mol. Sci.* **23**, 805 (2022).
33. Mignon, A. et al. Alginate biopolymers: Counteracting the impact of superabsorbent polymers on mortar strength. *Constr. Build. Mater.* **110**, 169–174 (2016).
34. Wondu, E., Lee, G. & Kim, J. Polybutylene adipate terephthalate (PBAT) composites for thermally conductive, fire retardant, high dielectric applications using BaTiO₃ and MWCNTs as fillers. *Polym. Test.* **135**, 108447 (2024).
35. Karthikeyan, R. & Madhu, S. Impact of brown algae particles on the mechanical properties of jute-reinforced polymeric composites for sustainable development. *Res. Eng.* **25**, 104548 (2025).
36. Gondim, F. F., Rodrigues, J. G. P., Aguiar, V. O., de Fátima Vieira Marques, M. & Monteiro, S. N. Biocomposites of cellulose isolated from coffee processing by-products and incorporation in poly(Butylene Adipate-Co-Terephthalate) (PBAT) matrix: An overview. *Polymers* **16**, 314 (2024).
37. Zhou, S. J. et al. A high-performance and cost-effective PBAT/Montmorillonite/Lignin ternary composite film for sustainable production. *ACS Sustain. Chem. Eng.* **12**, 14704–14715 (2024).
38. da Silva, T. C. P. et al. Development of biodegradable PLA/PBAT-based filaments for fertilizer release for agricultural applications. *Materials* **15**, 6764 (2022).
39. Sciancalepore, C. et al. Flexible PBAT-based composite filaments for tunable FDM 3D printing. *ACS Appl. Bio Mater.* **5**, 3219–3229 (2022).
40. Colucci, G., Lupone, F., Bondioli, F. & Messori, M. 3D printing of PBAT-based composites filled with agro-wastes via selective laser sintering. *Eur. Polym. J.* **215**, 113197 (2024).

Acknowledgements

The authors would like to express their gratitude to the Department of Bio-composite Laboratory, Institute of Tropical Forestry and Forest Products, Universiti Putra Malaysia for providing instrumental support for this project.

Author contributions

Data curation, Hamdan AH, Sarmin SN, Salim N and Jawaid M; Formal analysis, Sarmin SN, Ismail AS and Jawaid M; Funding acquisition, Sarmin SN and Salim N; Project administration, Sarmin SN and Jawaid M; Writing—original draft, Hamdan AH, Sarmin SN, and Zoheb K; Writing—review & editing, Hamdan AH, Sarmin SN, and Zoheb K, All authors have read and agreed to the published version of the manuscript.

Funding

The authors are thankful to United Arab Emirates University for funding this project through Grant No: 12R301 and 12R287.

Competing interests

The authors declare no competing interests.

Consent for publication

We confirm that this work is original and has not been published elsewhere, nor is it currently under consideration for publication elsewhere.

Ethical approval

No ethical clearance is required.

Human and animal rights

We declare that there are no animal studies or human participant involvement in the study.

Additional information

Correspondence and requests for materials should be addressed to M.J.

Reprints and permissions information is available at www.nature.com/reprints.

Publisher's note Springer Nature remains neutral with regard to jurisdictional claims in published maps and institutional affiliations.

Open Access This article is licensed under a Creative Commons Attribution-NonCommercial-NoDerivatives 4.0 International License, which permits any non-commercial use, sharing, distribution and reproduction in any medium or format, as long as you give appropriate credit to the original author(s) and the source, provide a link to the Creative Commons licence, and indicate if you modified the licensed material. You do not have permission under this licence to share adapted material derived from this article or parts of it. The images or other third party material in this article are included in the article's Creative Commons licence, unless indicated otherwise in a credit line to the material. If material is not included in the article's Creative Commons licence and your intended use is not permitted by statutory regulation or exceeds the permitted use, you will need to obtain permission directly from the copyright holder. To view a copy of this licence, visit <http://creativecommons.org/licenses/by-nc-nd/4.0/>.

© The Author(s) 2026